Cancellation of Motion Artifact Induced by Exercise for PPG-Based Heart Rate Sensing

Takunori Shimazaki, Shinsuke Hara, *Member, IEEE,* Hiroyuki Okuhata, *Member, IEEE,*
Hajime Nakamura, Takashi Kawabata

***Abstract*—Heart rate (HR) sensing during exercise is essential for medical, healthcare and sport physiological purposes. Photo-Plethysmo-Graphy (PPG) is a simple and non-invasive technique for HR sensing, but it is highly sensitive to motion artifact. This paper proposes a cancellation technique of motion artifact in PPG-based HR sensing for a man during exercise. The canceller is equipped with two sensors; one is a normal PPG sensor where an LED/Photo-Detector (PD) contacts the skin to detect Blood Volume Pulse (BVP) (+motion artifact) and the other is a motion artifact sensor where an LED/PD does not contact the skin to detect only motion artifact. Experimental results show that the proposed technique, which is implemented in adaptive algorithms, can sense HR correctly by cancelling motion artifact induced by exercises such as running and jumping.**

I. Introduction

Heart rate (HR) sensing during exercise is essential for preventing disease and injury, checking physical condition, and evaluating physical strength. For example, the Karvonen equation [1] requires real-time HR sensing to calculate adequate training strength for persons during exercises. We have developed a real-time vital signs collection system which senses vital signs such as HR, Energy Expenditure (EE) and Body Temperature (BT) by vital sensor nodes put to players in a field and wirelessly transmits their data to a note PC by a coach or trainer. We have implemented prototype vital sensor nodes [2] and have evaluated their sensing and transmission performances in field experiments conducted during 90-minite football games [3].

We can easily sense BT by contacting a thermistor to the skin and calculate EE using tri-accelerometer data [4]. To calculate EE only through walking, running and jumping, we want to put a tri-accelerometer somewhere to the lower half of the body, on the other hand, we want to put a HR sensor closer to the heart. We decided to sense HR, EE and BT commonly by a single sensor node put at the back-waist position of a person, so the HR sensing became very difficult, because there is no thicker artery under the skin.

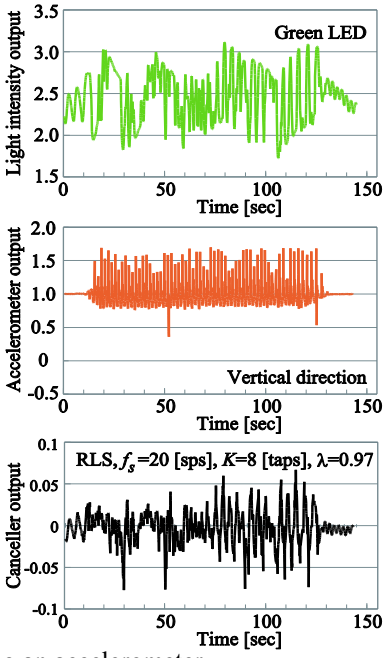

(a) using an accelerometer

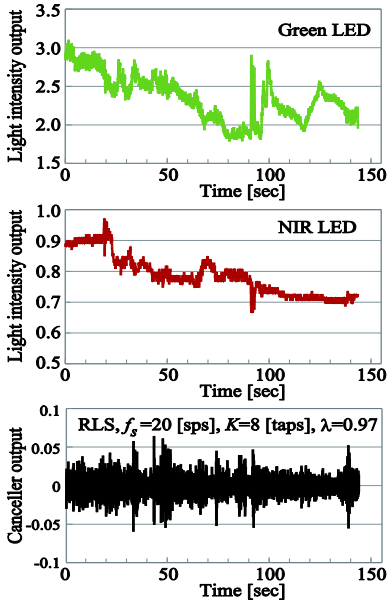

(b) using a NIR LED

Figure 1 performance of conventional artifact cancellers.

Manuscript received on March 17, 2014.

T. Shimazaki is with the Graduate School of Engineering, Osaka City University, 3-3-138, Sugimoto, Sumiyoshi-ku, Osaka 558-8585, Japan (phone: +81-6-6605-2795; fax: +81-6-6605-2795; e-mail: shimazaki @c.info.eng.osaka-cu.ac.jp).

S. Hara is with the Graduate School of Engineering, Osaka City University, 3-3-138, Sugimoto, Sumiyoshi-ku, Osaka 558-8585, Japan.

H. Okuhata is with Synthesis Corporation, 2-6-9, Awajimachi, Chuo-ku, Osaka 541-0047, Japan .

H. Nakamura is with the Graduate School of Medicine, Osaka City University, 1-5-17 Asahimachi, Abeno-ku, Osaka 545-0051, Japan.

T. Kawabata is with the School of Health and Well-being, Kansai University, 1-11-1 Kaorigaokachou, Sakai-ku, Sakai 590-8515 Japan.

978-1-4244-7929-0/14/$26.00 ©2014 IEEE

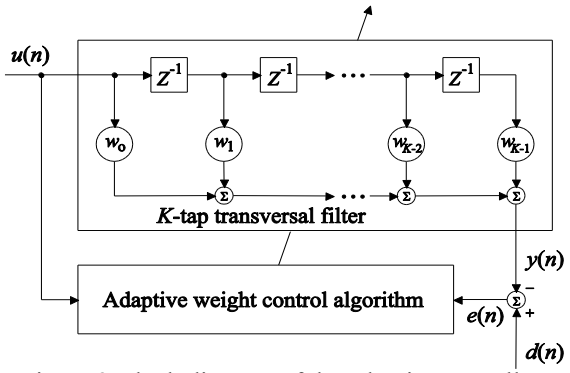

Figure 2 Block diagram of the adaptive canceller.

Among HR sensing methods, Photo-Plethysmo-Graphy (PPG) is based on opto-electronic technique, which illuminates the skin and measures the intensity of the light changed by the blood volume pulse (BVP) under the skin. PPG is a simple, unobtrusive and non-invasive technique for HR sensing suited for persons during exercises, but it is highly sensitive to motion artifact. Especially, when a sensor wearer takes hard exercise, the spectral component of motion artifact overlaps with that of BVP in PPG output, so a nonlinear technique is required to cancel the motion artifact. Figure 1 shows the performances of conventional motion artifact cancellers; using a green Light Emitting Diode (LED) and an accelerometer [5] (a) and using a green LED and a Near Infrared Red (NIR) LED [6] (b). We can see from this figure that the conventional techniques do not work well for the case of waist position HR sensing during exercise (see Section III in more detail).

This paper proposes a cancellation technique of motion artifact for PPG-based HR sensing. The canceller has inputs from two sensors; one is a normal PPG sensor, which detects BVP+motion artifact and the other is a sensor called "motion artifact sensor," which can detect only motion artifact. The cancellation performance is confirmed by experiments with three subjects during fast walking, running and jumping.

II. Adaptive Canceller

Figure 2 shows the block diagram of the adaptive canceller [7], which is composed of a K-tap transversal filter and an adaptive weight control algorithm. It also has two inputs, which is adequately sampled in f_s samples per second [sps]; one is from the normal PPG sensor $d(n)$ (n=0, 1, 2, …) and the other from the motion artifact sensor $u(n)$ (n=0, 1, 2, …). Defining the tap weight vector $_{(K\times 1)}$ and input vector of the transversal filter $_{(K\times 1)}$ respectively as

$$\mathbf{w} = [w_0, \ldots, w_{K-1}]^T \tag{1}$$

$$\mathbf{u}(n) = [u(n-K+1), \ldots, u(n)]^T \tag{2}$$

the transversal filter output is given by

$$y(n) = \mathbf{w}^T \mathbf{u}(n)\,. \tag{3}$$

In principle, the adaptive canceller algorithm tries to make the error between $d(n)$ and $y(n)$ be zero, but it should be noted

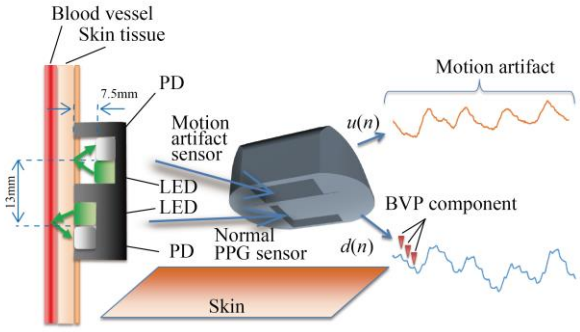

Figure 3 Principle of the proposed technique.

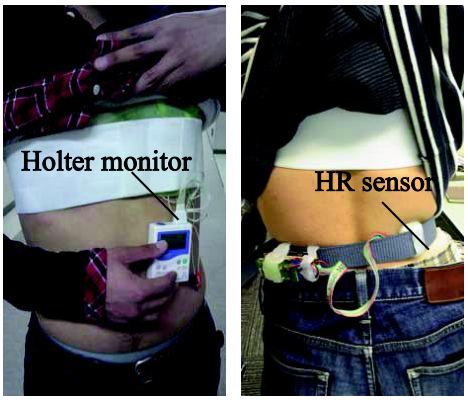

Figure 4 A subject with a Holter monitor and an HR sensor.

that the BVP component is obtained in the canceller output as "a residual error." Therefore, if the sampling rate is higher and the number of taps is larger, the canceller output contains a smaller BVP component as it can better cancel not only the motion artifact but also the BVP component using the output of the motion artifact sensor. This means that choice of the sampling rate and the number of taps is important. We apply the following two adaptive algorithms for the motion artifact cancellation.

A. NLMS Algorithm

The Normalized Least Mean Squares (NLMS) algorithm updates the weight vector as (n=0, 1, …) [7]

$$\mathbf{w}(n+1) = \mathbf{w}(n) + \frac{\mu}{\left\|\mathbf{u}(n)\right\|^2}\mathbf{u}(n)e(n) \tag{4}$$

$$e(n) = d(n) - y(n) \tag{5}$$

where μ is a parameter controlling the rate of convergence and residual error.

B. RLS Algorithm

On the other hand, the Recursive Least Squares (RLS) algorithm updates the weight vector as (n=0, 1, …) [7]

$$\boldsymbol{\pi}(n+1) = \mathbf{P}(n)\mathbf{u}(n+1) \tag{6}$$

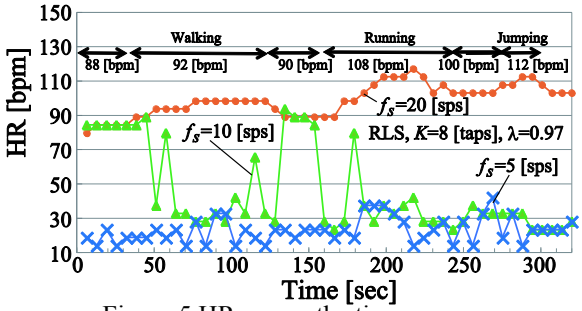

Figure 5 HR versus the time.

$$\mathbf{k}(n+1) = \frac{\boldsymbol{\pi}(n+1)}{\lambda + \mathbf{u}^T(n+1)\boldsymbol{\pi}(n+1)} \tag{7}$$

$$\xi(n+1) = d(n+1) - \mathbf{w}(n)^T \mathbf{u}(n+1) \tag{8}$$

$$\mathbf{w}(n+1) = \mathbf{w}(n) + \mathbf{k}(n+1)\xi(n+1) \tag{9}$$

$$\mathbf{P}(n+1) = \lambda^{-1}\mathbf{P}(n) - \lambda^{-1}\mathbf{k}(n+1)\mathbf{u}^T(n+1)\mathbf{P}(n) \tag{10}$$

with $\mathbf{w}(0)=\mathbf{0}$ and $\mathbf{P}(0)=10^{-3}\mathbf{I}$, where λ is a forgetting factor.

III. Motion Artifact Sensor

The key is how correctly the motion artifact sensor can detect only motion artifact. An accelerometer signal is considered to be correlated with motion artifact. In Figure 1 (a), an accelerometer (vertical direction) was used as a motion artifact sensor, but in our experiment, the motion artifact was not cancelled because the correlation between them was low. On the other hand, the penetration depth of light depends on its wavelength [8]. That of NIR light (940 [nm]) is longer enough to reach vascular bed located deeper under the skin whereas that of green light (520 [nm]) is shorter. In Figure 1 (b), a green LED/PD was used as a motion artifact sensor, but in our experiment, the motion artifact was not cancelled because both the PPG sensor and motion artifact sensor detected the BVP component.

In PPG, usually both an LED and a Photo Detector (PD) contact the skin to detect stronger light reflected by vascular bed. Through a lot of experiments and measurements, we finally found that when an LED/PD does not contact the skin, in other words, there is an air gap between an LED/PD and the skin, the PD detects only motion artifact. Figure 3 shows the principle of out proposed technique. It uses two LED/PDs; one is a normal PPG sensor where an LED/PD contacts the skin to detect BVP component (and inevitably motion artifact) and the other is a motion artifact sensor where an LED/PD does not contact the skin (the air gap height is 7.5 [mm]) to detect only motion artifact. The locations of the two sensors should be closer (the distance is 13.0 [mm]) to make the motion artifact detected by the motion artifact sensor be more correlated with that of the PPG sensor. The same green LEDs are used for the two sensors, because it is advantageous to detect light reflected by capillary vascular bed located shallower under the skin of the back and the motion artifacts detected by the two sensors should be more correlated.

Table 1 RMSE of HR for the NLMS algorithm.

K [taps] \ μ	0.1	0.5	0.7
10	20 [bpm]	20 [bpm]	22 [bpm]
30	8 [bpm]	5 [bpm]	10 [bpm]
50	9 [bpm]	9 [bpm]	12 [bpm]
80	8 [bpm]	5 [bpm]	11 [bpm]

Table 2 RMSE of HR for RLS algorithm.

K [taps] \ λ	0.95	0.97	0.99
10	23 [bpm]	16 [bpm]	13 [bpm]
30	15 [bpm]	12 [bpm]	8 [bpm]
50	14 [bpm]	11 [bpm]	6 [bpm]
80	19 [bpm]	15 [bpm]	11 [bpm]

IV. Experimental Setup

First, we conducted a preliminary experiment with a subject, the aim of which was to adequately choose the sampling rate f_s the number of taps K and the adjustable parameters μ or λ for each adaptive algorithm. In the experiment, we put an HR sensor composed of a normal PPG sensor and a motion artifact sensor to the back-waist position of the subject and he performed one-minute standing still (resting), two-minute walking (4 kilometers per hour [km/h]), one-minute standing still, two-minute running (10 [km/h]), one-minute standing still and two-minute jumping. During the experiment, the sensed data were stored in an SD card memory, and after the experiment, the data were processed offline.

Then, we conducted a final experiment with three subjects. In the experiment, we put an HR sensor to the back-waist position of each subject and at the same time put a Holter monitor to the chest position of the same subject. Figure 4 shows a subject with a Holter monitor and an HR sensor. One experimental session is composed of four times of one-minute standing still (rest) and two-minute fast walking, running or jumping. Each subject repeated the session four times in total. During the experiment, the sensed data were also stored by a SD card memory, and after the experiment, the data were processed offline by the cancellation algorithms. Note that we also processed the data by means of the Least Mean Square (LMS) algorithm, but the motion artifact was not cancelled.

V. Results and Discussions

A. Sampling Rate

Figure 5 shows the HR in beats per minute [bpm] versus the time for the sampling rates of 5 [sps], 10 [sps] and 20 [sps]. In the figure, the average HRs are also shown. The sampling rate should be lower to reduce the data volume and the Central Processing Unit (CPU) load. From the figure, we can see that the sampling rate of 20 sps is an adequate choice.

B. *Number of Taps and Adjustable Parameters for NLMS and RLS Algorithms*

Table 1 and 2 summarize the Root Mean Square Error (RMSE) of HR for the NLMS and RLS algorithms, respectively. In the NLMS algorithm, for each of the number of taps, there seems an optimal value in μ which can minimize the RMSE, on the other hand, in the RLS algorithm, for each of the number of taps, a larger value of λ can reduce the RMS. For the tables, we can see that a set of K=30 and μ=0.5 is an adequate choice for the NLMS algorithm and a set of K=50 and λ=0.99 is an adequate choice for the RLS algorithm.

C. *RMSE of HR for fast-walking, running and jumping*

Figures 6 (a), (b) and (c) show the HR versus the time for the cases of fast-walking, running and jumping, respectively, which was obtained from the result of subject A. In these figures, the performances of the Holter monitor are considered to be reference. For comparison purpose, these figures also contain the performances of a linear motion artifact canceller, that is, a band-pass filtering (BPF) of 0.8 to 3.0 [Hz]. We can see from these figures that for the three exercises, the linear canceller does not work well at all, but our proposed canceller works very well; the performance is almost the same as that of the Holter Monitor. From the figures, running seems the most adverse exercise for the HR sensing among the three.

Finally, Table 3 compares the RMSEs among the BFP, the NLMS-based canceller and the RLS-based canceller, which were averaged over the three subjects. The performance of the NLMS algorithm is comparable to that of the RLS algorithm. The computational complexity of the NLMS algorithm is much lower than that of the RLS algorithm, so from the overall result, we can conclude that the NLMS algorithm is the best choice for the proposed motion artifact canceller.

VI. Conclusions

This paper has proposed a motion artifact cancellation technique for PPG-based hart rate sensing. Its principle is simple, it has just one LED/PD which contacts the skin to detect the BVP and the other LED/PD which does not contact the skin to detect only motion artifact. The cancellation works well for motion artifact induced by fast walking, running and jumping. In the experimental result, the performance of using the NLMS algorithm is comparable to that of using the RLS algorithm.

Acknowledgement

This research was partly supported by the Strategic Information and Communications R&D Promotion Programme (SCOPE, No. 122307002) of the Ministry of Internal Affairs and Communications of Japan, and the Support Center for Advanced Telecommunications Technology Research, Foundation (SCAT).

References

[1] M. Karvonen, K. Kentala, and O. Mustala, "The effects of training on heart rate: a longitudinal study," Ann Med Exp Biol Fenn, vol. 35, no. 3, pp. 307-315, 1957.

[2] S. Okamoto et al., "Design of Wireless Waist-Mounted Vital Sensor Node for Athletes -Performance Evaluation of Microcontrollers Suitable for Signal Processing of ECG Signal at Waist Part-," Proc. IEEE Radio & Wireless Week (RWW) 2014, in CD-ROM, Newport Beach, USA, 19-22 Jan. 2014.

[3] S. Hara et al., "Development of a Real-Time Vital Data Collection System from Players during a Football Game," accepted for presentation at IEEE International Conference on e-Health Networking, Applications and Services (Healthcom) 2013, in CD-ROM, Lisbon, Portugal, 9-12 Oct. 2013.

[4] K. Nemoto et al., "Effects of High-Intensity Interval Walking Training on Physical Fitness and Blood Pressure in Middle-Aged and Older People," Mayo Clinic Proceedings, Vol. 82, No. 7, pp. 803-811, July 2007.

[5] H. Fukushima et al., "Estimating Heart Rate Using Wrist-type Photoplethysmography and Acceleration Sensor While Running," Proc. IEEE EMBC 2012, pp. 2901-2904, San Diego, USA, 28 Aug.-1. Sep. 2012.

[6] Japan Patent, "A Mobile Vital Information Monitor and Management Device (in Japanese)," JP-110921A, Apr. 2005.

[7] S Haykin, Adaptive Filter Theory, Fourth Edition, Prentice Hall, 2002.

[8] Y. Maeda et al," Comparison of Reflected Green Light and Infrared Photoplethysmography," Proc. IEEE EMBC 2008, pp. 2270-2272, Vancouver, Canada, 20-24 Aug. 2008.

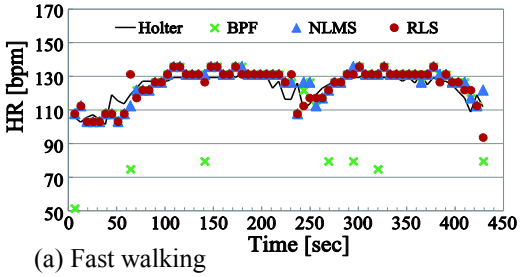

(a) Fast walking

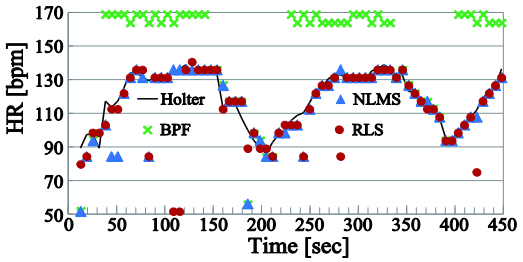

(b) Running

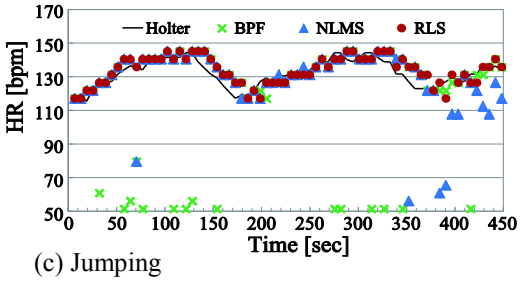

(c) Jumping

Figure 6 HR versus the time (subject A).

Table 3 RMSE (averaged) of the cancellers.

Canceller / Exercise	BPF	NLMS	RLS
Fast walking	17 [bpm]	8 [bpm]	10 [bpm]
Running	38 [bpm]	18 [bpm]	15 [bpm]
Jumping	40 [bpm]	19 [bpm]	19 [bpm]